AIAA Guidance, Navigation, and Control Conference and Exhibit
11-14 August 2003, Austin, Texas

AIAA 2003-5507

PERFORMANCE EVALUATION OF RENDEZVOUS USING MODEL PREDICTIVE CONTROL

Arthur Richards* and Jonathan How†

ABSTRACT

A new form of Model Predictive Control (MPC) is presented. It is shown to guarantee robust, finite-time maneuver completion for an arbitrary target region. The new method is used to control spacecraft rendezvous and its performance is compared, in simulation, with both a traditional, glideslope approach and an earlier MPC formulation. The new method is shown to use less fuel than both other controllers. The development over existing MPC formulations is the ability to explicitly minimize fuel cost for a general target point, not necessarily an equilibrium. The new formulation also guarantees robust completion of the maneuver. Given an unknown but bounded disturbance, the spacecraft will still reach the target in finite time. This is demonstrated in simulation, also showing that the new formulation of MPC offers lower fuel use than the glideslope algorithm when unmodeled disturbances are present.

INTRODUCTION

This paper extends a recently-developed form of Model Predictive Control (MPC) [2] to guarantee robust, finite-time maneuver completion. The resulting controller is then applied to the problem of spacecraft rendezvous. This demonstrates two key features of the new MPC method. Firstly, its ability to handle a general target region, not necessarily enclosing an equilibrium, offers performance benefits over existing MPC forms. Secondly, the robustness modifications ensure that the maneuver is completed in finite time in the presence of an unknown, but bounded, disturbance. Overall, it is shown that MPC uses significantly less fuel to perform rendezvous than the commonly-used glideslope approach controller.

MPC is an emerging technology [9] involving the repeated solution of an optimal control problem. An initial portion of the resulting control sequence is implemented and then the problem is solved again, starting from the new state. In this way, MPC combines both feedforward and feedback control. The primary advantage of MPC is the explicit awareness of constraints in the controller, allowing the closed-loop system to operate closer to the boundaries of its region of operation and thus achieving better performance than more traditional schemes [9]. This comes at the expense of a more complicated computation, which must be performed on-line in real-time. MPC has been successfully adopted in the process control industry, where dynamics are comparatively slow. However, applications in aerospace are only recently forthcoming [21, 15], enabled by the on-going development of faster computers. Recent work on parametric solution of MPC optimizations [17, 18] also enables application to faster systems.

Existing forms of MPC require either that the target is an unforced equilibrium [16] or that the cost function penalizes the difference between the control inputs and the equilibrium forcing required to remain at the target [10]. For example, consider a spacecraft approaching a point radially-separated from a space station. The target point is not a natural equilibrium, so if fuel is used as the cost function, the controller will fail to complete the maneuver. When the cost function is modified to guarantee stability, the results are no longer fuel-optimal, and the performance suffers. The new formulation extends previous work [2, 22] in which a variable horizon was used to achieve stability. Here, MILP optimization is used to effect a variable horizon length, leading to guaranteed finite-time completion.

MILP has been used for open-loop vehicle trajectory design, enabling the inclusion of non-convex constraints such as collision avoidance and plume impingement avoidance [11]. Powerful, commercial computation tools exist for the solution of MILP problems [12, 13] and its use for MPC has been considered theoretically [10, 2] in terms of stability. This paper provides quantitative results of the performance benefits attainable.

The second development of this paper is the guarantee of *robust completion*. This extends the au-

* Research Assistant, MIT Dept. of Aeronautics and Astronautics, **arthurr@mit.edu**
† Associate Professor, MIT Dept. of Aeronautics and Astronautics, **jhow@mit.edu**. MIT 33-328, 77 Mass. Ave., Cambridge, MA 02139

Copyright © 2003 by the American Institute of Aeronautics and Astronautics, Inc. All rights reserved.

thors' previous work on *robust feasibility* [2]. Assuming that the disturbance is bounded, the optimization can be modified such that the optimal cost of each new plan is less than that of the previous plan by at least some known, non-zero amount. Then the property of finite-time completion is retained. This is demonstrated in simulations including disturbances.

Many proposed space systems require autonomous rendezvous capability [3, 4], including ISS supply craft like ATV and HTV [1] and on-orbit servicing missions such as Orbital Express [5]. To date, the most popular control scheme for rendezvous is the glideslope approach [8], in which the chaser vehicle moves along a straight line towards its target. Controlled by a human operator, this has been used successfully many times, from the Apollo era to modern shuttle/ISS missions [6]. Ref. [7] describes an automated version of the glideslope approach for unmanned vehicles. Besides proven heritage, the advantages of the glideslope approach include a continuous line-of-sight to target and relatively light online computation requirements. These come at the expense of obvious fuel penalties, since a straight line approach requires actuation against the force of gravity. In the past, the benefits have justified the fuel costs. In this paper, the glideslope algorithm is used as a performance baseline for comparison with MPC.

The paper begins with a description of the two test cases used for comparison. Then a review of the formulations is presented, including their configurations for the simulations. The first set of simulations compares the glideslope algorithm with the two MPC methods in the absence of disturbance, showing the performance benefit of the variable horizon MPC method. The second set of simulations includes disturbances and demonstrates the new robust MPC method, comparing performance with the glideslope algorithm.

TEST CASE DESCRIPTION

Two test cases were used for the comparison: (A) intrack approach and (B) radial approach. These represent approaches to two different docking ports on the ISS. Fig. 1 shows a notional space station model and the two approach regions. The station is modeled in a circular orbit with a period of 90 minutes. The relative reference frame has its x-axis pointing radially outwards, its y-axis extending forward along the orbit and its z-axis forming a right-handed set in the out-of-plane direction. The Hills-Clohessy-Wiltshire (HCW) equations [19] are used as the model of the relative dynamics.

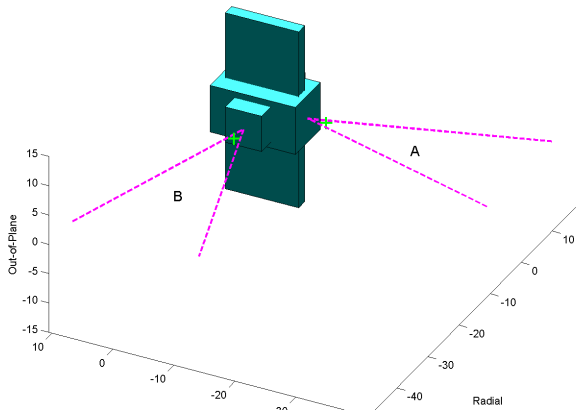

Fig. 1: Approach Test Cases

The target points, marked by crosses in Fig. 1, are $(0, -10, 0)$ for case A, *i.e.* approaching from behind, and $(-10, 0, 0)$ for case B, *i.e.* approaching from below. Typically, these points would be close to the docking port and a separate, final approach controller would complete the physical docking. For both cases, the starting state is 70 m away along the direction of approach: $(0, -80, 0)$ for A and $(-80, 0, 0)$ for B. The chaser vehicle is modeled as a point mass, neglecting attitude, with impulsive actuation of up to 0.09 m/s in each direction. To represent a proximity safety constraint, its relative velocity is limited to less than 0.07 m/s in each direction.

Target visibility is frequently cited as a major advantage of the glideslope method. Since the chaser moves along a nearly-straight path from the starting point to the target, a line-of-sight to the target is always maintained. This is crucial if, for example, cameras are used as the relative position sensors. To capture this feature in MPC, explicit visibility constraints are included to ensure that the chaser remains within the field of view of some notional sensor. The constraints in each case form a wedge, with half angle 16.7^o and apex 3 m beyond the target point. The visibility constraint boundaries are shown dashed in Fig. 1.

The first set of simulations do not include any disturbances. In the second set, a combination of constant and random disturbance was added. A constant acceleration of $6.67\text{x}10^{-6}$ m/s^2 in the intrack direction represents the effect of atmospheric drag. A further random acceleration, uniformly chosen with magnitude up to $6.67\text{x}10^{-6}$ m/s^2 in each direction, represents random effects such as actuation error or model-mismatch. The disturbances are implemented as additional ΔV on each control ac-

tuation, with magnitude suitably-scaled for the time step length.

CONTROLLER FORMULATIONS

This section describes the formulation and configuration of the controllers used. The glideslope algorithm is not reviewed, for brevity, but its configuration is described. A fixed-horizon MPC (FH-MPC) formulation is then presented, to be used for comparison in simulations. Next, the new variable-horizon MPC (VH-MPC) formulation is presented. Finally, the modifications for robustness are shown, referred to as "Robust Variable-Horizon MPC" (RVH-MPC)

Glideslope Algorithm

The glideslope algorithm is described in detail in Refs. [7, 8]. For this test, the maneuvers are performed with twelve firing pulses, aiming for a closing rate of approach of 2cm/s. The initial approach rate was adjusted to give a completion time similar to that for the VH MPC method (see later). This led to initial approach rate settings of 8cm/s for the radial approach and 3.5cm/s for the in-track.

Fixed-Horizon MPC (FH-MPC)

The fixed-horizon MPC formulation is described in detail in Ref. [10]. At each time step k, the model predictive control problem is to design an input sequence $\{\mathbf{u}_{k|k} \dots \mathbf{u}_{k|(k+N)}\}$ and corresponding state sequence $\{\mathbf{x}_{k|k} \dots \mathbf{x}_{k|(k+N+1)}\}$ for the horizon N, where $\mathbf{u}_{k|j}$ denotes the control designed at time step k for application at time step j. Then the first element of that sequence is applied. The optimization includes a model of the dynamics

$$\forall j \in [k \dots (k+N)]\ \mathbf{x}_{\mathrm{k|(j+1)}} = \mathbf{A}\mathbf{x}_{\mathrm{k|j}} + \mathbf{B}\mathbf{u}_{\mathrm{k|j}} \quad (1)$$

where $\mathbf{A}$ and $\mathbf{B}$ are the discretized system matrices for the HCW equations, using the modeled orbit period of 90 minutes and a time step length of 150 s. The horizon was set at $N = 18$ steps, equivalent to half the orbital period.

The terminal condition is found by solving for the terminal velocity and thrust consistent with remaining at the required position. Note that the terminal velocity is non-zero since the system has been discretized for an impulsive ΔV actuation. The target state is partitioned into position and velocity $(\mathbf{r}_T\ \mathbf{v}_T)$, where $\mathbf{r}_T$ is the desired target. Accordingly, the state transition matrices are partitioned into 3×3 blocks $\mathbf{A}_{\mathrm{i}}$ and $\mathbf{B}_{\mathrm{i}}$. Then the condition for equilibrium of the discrete system is

$$\begin{pmatrix} \mathbf{r}_T \\ \mathbf{v}_T \end{pmatrix} = \begin{bmatrix} \mathbf{A}_1 & \mathbf{A}_2 \\ \mathbf{A}_3 & \mathbf{A}_4 \end{bmatrix} \begin{pmatrix} \mathbf{r}_T \\ \mathbf{v}_T \end{pmatrix} + \begin{bmatrix} \mathbf{B}_1 \\ \mathbf{B}_2 \end{bmatrix} \mathbf{u}_{eq} \quad (2)$$

This can be re-written as

$$\begin{bmatrix} \mathbf{A}_2 & \mathbf{B}_1 \\ (\mathbf{A}_4 - \mathbf{I}) & \mathbf{B}_2 \end{bmatrix} \begin{pmatrix} \mathbf{v}_T \\ \mathbf{u}_{eq} \end{pmatrix} = \begin{bmatrix} (\mathbf{I} - \mathbf{A}_1) \\ -\mathbf{A}_3 \end{bmatrix} \mathbf{r}_T \quad (3)$$

which can be solved for $\mathbf{v}_T$ and $\mathbf{u}_{eq}$ given $\mathbf{r}_T$. The terminal constraint is

$$\mathbf{x}_{\mathrm{k|N+1}} = \begin{pmatrix} \mathbf{r}_T \\ \mathbf{v}_T \end{pmatrix} \quad (4)$$

The initial conditions are taken from the current state values

$$\mathbf{x}_{\mathrm{k|k}} = \mathbf{x}_{\mathrm{k}} \quad (5)$$

Other constraints are physical limits on the actuation and the safety limits on the velocity, $|\mathbf{u}| \leq \bar{U}$, safety limits on the velocity, $|\mathbf{v}| \leq \bar{V}$, and the visibility constraints. These are all included in the following general form

$$\begin{gathered} \forall j \in [k \dots (k+N)] \\ \mathbf{C}_1\mathbf{x}_{\mathrm{k|j}} + \mathbf{C}_2\mathbf{u}_{\mathrm{k|j}} + \mathbf{C}_3 \geq \mathbf{0} \end{gathered} \quad (6)$$

To apply non-convex constraints, such as collision avoidance or plume impingement prevention, auxiliary binary variables could also be included in (6).

The objective function is the one-norm of the difference between each input and the equilibrium value.

$$J^* = \min_{\{\mathbf{x},\mathbf{u}\}} \sum_{\mathrm{j=k}}^{(k+N)} |\mathbf{u}_{\mathrm{k|j}} - \mathbf{u}_{eq}| \quad (7)$$

The cost can be realized in linear form using slack variables. The complete stability proof is given in Ref. [10]. It relies on the fact that executing the control $\mathbf{u}_{eq}$ incurs no cost. Therefore, at each step, a solution to the new trajectory optimization is the continuation of the previous plan. The optimal cost can then be used as a Lyapunov function to show stability. In summary, the MPC scheme is as follows:

1. Solve the minimization of (7) subject to constraints (1) and (4)–(6);
2. Apply first element of continuous control sequence $\mathbf{u}_{\mathrm{k|k}}$ to the vehicle;
3. Go to 1.

Variable-Horizon MPC (VH-MPC)

The formulation in this section was introduced in Ref. [2]. Whereas the formulation in the previous section has a single target point, the objective of this formulation is to steer the state $\mathbf{x}$ into the region defined by $\mathbf{P}\mathbf{x} \leq \mathbf{q}$. Typically, this will define some "box" in the state-space. In this case, it constrains a

region lying within 0.1 m of the target point. It also limits the final velocity to less than 1 mm/s in any direction. The aim is only to reach that region: it is not necessary for this controller to keep the state there. This would be accomplished by another system such as physical docking or a finer tolerance, final approach controller.

The system state is subject to the same dynamic constraints (1) as in the previous section. In this optimization model, the system state is augmented with a single discrete state, $y \in \{0, 1\}$, where $y = 0$ is defined to imply that the target has been reached at the current step or earlier, and $y = 1$ implies that the target has yet to be reached. The dynamics of y are described by a discrete-time state-space model

$$\forall j \in [k \dots (k+N)] \; y_{\mathrm{k|(j+1)}} = y_{\mathrm{k|j}} - v_{\mathrm{k|j}} \tag{8}$$

where $v \in \{0, 1\}$ is a discrete input. The input sequence $\{v_{k|k} \dots v_{k|(k+N)}\}$ is an additional decision variable in the optimization, subjected to the following constraint

$$\begin{gathered} \forall j \in [k \dots (k+N)] \\ \mathbf{P}(\mathbf{A}\mathbf{x}_{\mathrm{k|j}} + \mathbf{B}\mathbf{u}_{\mathrm{k|j}}) \leq \mathbf{q} + \mathbf{1}M(1 - v_{\mathrm{k|j}}) \end{gathered} \tag{9}$$

where $\mathbf{1}$ is a vector of suitable size whose entries are one and M is a large positive integer. If $v_{\mathrm{k|j}} = 1$, the target region constraint is met at the step $j + 1$, otherwise the constraint is relaxed. Also, if $v_{\mathrm{k|j}} = 1$, the discrete state y makes the transition from 1 to 0 between steps j and $j + 1$, according to (8). Therefore, the model of the discrete state is consistent with its definition: that $y = 0$ implies the target has been reached.

The operating constraints (6) are represented in the optimization in the following form

$$\begin{gathered} \forall j \in [k \dots (k+N)] \\ \mathbf{C}_1\mathbf{x}_{\mathrm{k|j}} + \mathbf{C}_2\mathbf{u}_{\mathrm{k|j}} + \mathbf{C}_3 + \mathbf{1}M(1 - y_{\mathrm{k|j}}) \geq \mathbf{0} \end{gathered} \tag{10}$$

in which the constraints are relaxed if $y = 0$. This relaxation of the constraints after completion of the problem means the plan incurs no cost after passing through the target. This is an important property for the proof of completion, discussed later in this section.

The initial condition of the continuous states is taken from the current state (5), as in the previous section. The discrete state is always initialized to 1, implying that the maneuver has yet to be completed.

$$y_{\mathrm{k|k}} = 1 \tag{11}$$

There is no terminal constraint on the continuous states. Therefore (4) is replaced by a constraint on the discrete state

$$y_{\mathrm{k|k+N+1}} = 0 \tag{12}$$

which implies that the system has passed through the terminal region at some point in the horizon, but need not be there at the horizon end itself.

The objective function is a combination of fuel and time. The cost function in the optimization is as follows

$$J^*(k) = \min_{\{\mathbf{x},\mathbf{u},y,v\}} \sum_{\mathrm{j=k}}^{(k+N)} (\gamma|\mathbf{u}_{\mathrm{k|j}}| + y_{\mathrm{k|j}}) \tag{13}$$

where γ is the fuel weighting. Since $y = 1$ until the maneuver is completed, the summation of y in the cost represents the planned time to completion, in units of time steps. In summary, the variable-time MPC scheme is as follows. At each time step:

1. Solve the minimization of (13) subject to constraints (1), (10) and (8)–(12);
2. Apply first element of continuous control sequence $\mathbf{u}_{\mathrm{k|k}}$ to the vehicle;
3. Go to 1.

The formal proof of nominal finite-time completion is given in Ref. [2]. Like FH-MPC, it is based on the fact that a feasible solution to each optimization is the continuation of the previous plan. Since the operating constraints (10) are relaxed once the target has been reached, it is always feasible to apply zero control $\mathbf{u} = \mathbf{0}$ for the additional step at the end of the new plan. Since the objective function includes a count of the time steps to completion, the optimization cost must decrease by at least one unit per time step. The cost is a positive definite quantity, with $J^*(k) = 0$ implying completion of the maneuver. Therefore, the maneuver will always be completed in fewer steps than the integer part of the first optimal cost, $\mathtt{int}(J^*(0))$.

Comparison of the two cost functions shows the root of the performance advantage of the new method. The cost for the fixed-horizon method (7) includes $\mathbf{u}_{eq}$, which is dependent on the terminal conditions. The cost for the variable-horizon method (13) always minimizes fuel, the true cost, even though the target region $\mathbf{P}\mathbf{x} \leq \mathbf{q}$ may not enclose a natural equilibrium. The importance of this distinction is shown in simulation later in the paper.

Robust Variable-Horizon MPC (RVH-MPC)

This section presents modifications to the VH-MPC formulation to guarantee robust completion *i.e.* that in the presence of a bounded disturbance, the maneuver will always be completed in a known, finite time. A disturbance input is included in the system model of (1) as follows

$$\mathbf{x}_{k+1} = \mathbf{A}\mathbf{x}_k + \mathbf{B}\mathbf{u}_k + \mathbf{B}_w\mathbf{w}_k \tag{14}$$

where $\mathbf{w}_k$ is an unknown disturbance, but bounded by $|\mathbf{w}_k| \leq \bar{W}$. Suppose the following optimal control sequence has been found at time step k

$$\begin{pmatrix} \mathbf{u}_{k|k} \\ \mathbf{u}_{k|(k+1)} \\ \mathbf{u}_{k|(k+2)} \\ \mathbf{u}_{k|(k+3)} \\ \vdots \\ \mathbf{u}_{k|(k+N-1)} \\ \mathbf{u}_{k|(k+N)} \end{pmatrix}$$

which has cost $J^*(k)$ and reaches the target at step j. The robustness technique ensures that the following plan, involving an immediate two-step correction to the disturbance, is a feasible solution at step $k+1$

$$\begin{pmatrix} \mathbf{u}_{k|(k+1)} + \delta\mathbf{u}_{(k+1)|(k+1)} \\ \mathbf{u}_{k|(k+2)} + \delta\mathbf{u}_{(k+1)|(k+2)} \\ \mathbf{u}_{k|(k+3)} \\ \vdots \\ \mathbf{u}_{k|(k+N)} \\ \mathbf{0} \end{pmatrix}$$

This still leads to completion at time j. Since the previous plan must have reached the target before time $k+N$, the additional zero control step at the end must be feasible, since the constraints (10) are relaxed after completion. The correction terms are given by [2]

$$\begin{bmatrix} \delta\mathbf{u}_{(k+1)|(k+1)} \\ \delta\mathbf{u}_{(k+1)|(k+2)} \end{bmatrix} = -[\mathbf{AB}\ \mathbf{B}]^{-1}\mathbf{A}^2\mathbf{B}_w\mathbf{w}_k \tag{15}$$

Since the system is two-step controllable, the matrix $[\mathbf{AB}\ \mathbf{B}]$ is invertible. Given the norm bound of $\mathbf{w}_k$, induced norms can be used to find bounds on the control corrections

$$\begin{aligned} |\delta\mathbf{u}_{(k+1)|(k+1)}| &\leq \beta_1 \\ |\delta\mathbf{u}_{(k+1)|(k+2)}| &\leq \beta_2 \end{aligned} \tag{16}$$

Fig. 2 shows how the control actuation is limited at future steps of the plan. At each new step, corrections of up to β_1 and β_2 in magnitude can be applied. Therefore, the plan comprised of the two step correction and the remainder of the previous plan is always feasible. The optimization will usually find a much better solution than the two step correction, but the existence of this solution guarantees feasibility. Note that similar constraint modifications must be applied to the state constraints: see Ref. [2] for details. Given that the corrected plan is a feasible solution to the optimization, its cost is an upper bound on the new optimal cost.

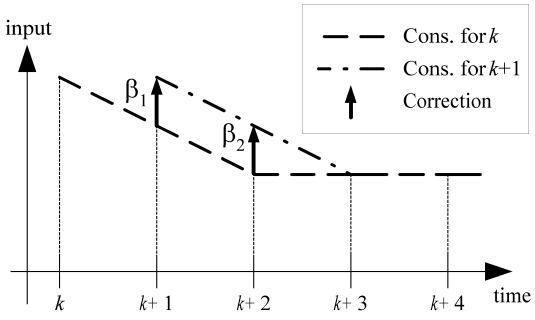

Fig. 2: Input Constraints for Robust Feasibility

$$\begin{aligned} J^*(k+1) \leq J^*(k) - 1 + \\ \gamma(|\delta\mathbf{u}_{(k+1)|(k+1)}| + |\delta\mathbf{u}_{(k+1)|(k+2)}|) \end{aligned} \tag{17}$$

where the decrement of one is due to the loss of a time step: both plans complete at step j. The additive term is the extra fuel cost for the correction, bounded using the triangle inequality

$$|\mathbf{u} + \delta\mathbf{u}| \leq |\mathbf{u}| + |\delta\mathbf{u}|$$

Given the limits in (16), a further bound can be derived.

$$J^*(k+1) \leq J^*(k) - 1 + \gamma(\beta_1 + \beta_2) \tag{18}$$

Therefore, if the fuel weighting γ is chosen such that the quantity $\lambda = 1 - \gamma(\beta_1 + \beta_2)$ is strictly positive, then the cost function must decrease by at least λ each time a plan is made and the target must be reached in fewer than $\texttt{int}(J^*(0)/\lambda)$ steps.

For the disturbance environment described in the 'Test Case Description' section, the disturbing acceleration can be bounded as no more than $1.33\text{x}10^{-5}$ m/s^2 in each direction. When the disturbance was included, the control actuation limits (as ΔV) were reduced by $\beta_1 = 0.0045$ m/s on the second step and a further $\beta_2 = 0.0025$ m/s on all steps thereafter (5% and 2.8% of available actuation respectively). For

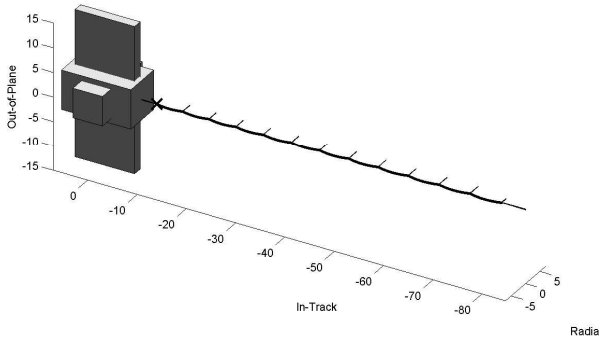

(a) Glideslope

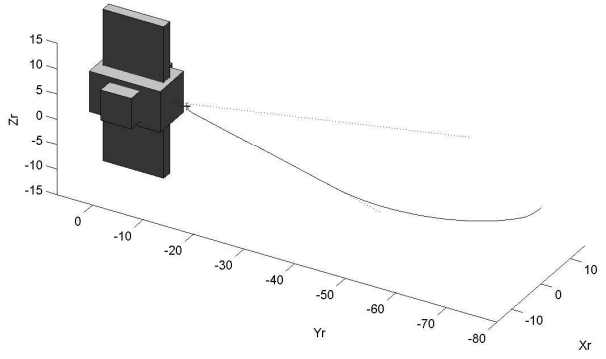

(b) VH-MPC

Fig. 3: Trajectories for Case A (in-track approach)

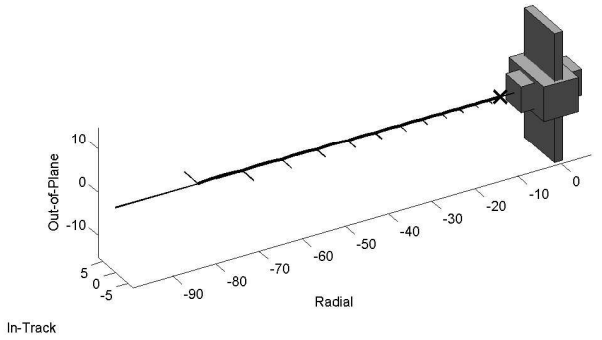

(a) Glideslope

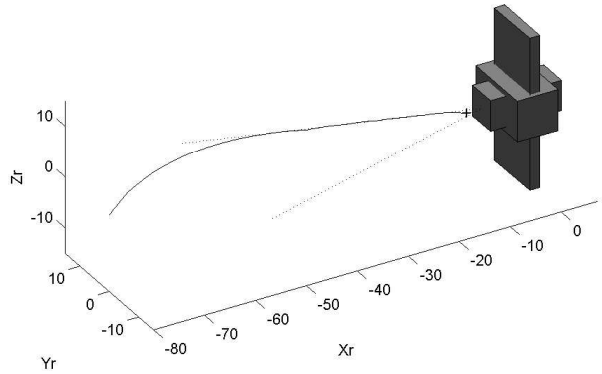

(b) VH-MPC

Fig. 4: Trajectories for Case B (radial approach)

the simulations with disturbance, the fuel weighting γ was set to 120, giving a minimum cost decrement $\lambda = 0.16$ and therefore satisfying the robust convergence criterion.

RESULTS

Figs. 3 and 4 show the trajectories from both VH-MPC and glideslope algorithm for both cases. The glideslope path remains close to a straight line approach, as intended. The VH-MPC approach moves to the limit of the visibility constraints. (FH-MPC trajectories look very similar to VH-MPC and are not shown.)

Comparison without Disturbance

This section compares FH-MPC with VH-MPC, to illustrate the performance differences, and then both with the glideslope algorithm. Table 1 shows the total fuel-use results of the three algorithms for both cases without the inclusion of disturbing forces in the simulations. Fig. 5 illustrates the results. The fuel weighting for VH-MPC was 900, emphasizing fuel cost over time. (Note that this is too high for the robust completion criterion and a different weighting is used in the next section.)

First compare the two MPC methods. For case A (the in-track approach), the two forms of MPC have roughly the same performance. Since the terminal point is along the in-track axis, it is a natural equilibrium. This makes the two methods equivalent: since $\mathbf{u}_{eq} = \mathbf{0}$, the two cost functions (7) and (13) are almost identical. The small time weighting in VH-MPC is the cause of its slightly higher (14%) fuel use. For case B (the radial approach), the two MPC approaches show significantly different performance. FH-MPC uses 35% more fuel than VH-MPC. The target for case B is not a natural equilibrium and $\mathbf{u}_{eq} \neq \mathbf{0}$. While the two methods have identical feasible sets of trajectories, VH-MPC minimizes $|\mathbf{u}|$, which still represents the true fuel cost, but FH-MPC minimizes $|\mathbf{u} - \mathbf{u}_{eq}|$. This mismatch in the minimized cost and the true cost causes the degra-

Table 1: Simulation Results without Disturbance. *ΔV in m/s

Controller	Case A ΔV*	Case B ΔV
Glideslope	0.207	0.456
FH-MPC	0.0748	0.422
VH-MPC	0.0853	0.313

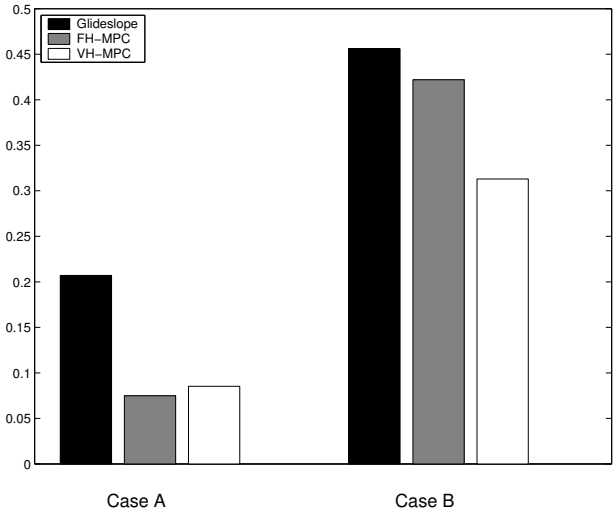

Fig. 5: Comparison of Fuel Use of Glideslope, FH-MPC and VH-MPC without Disturbance.

dation in performance of FH-MPC.

In both cases, the glideslope algorithm uses more fuel than either MPC form due to the "fight" with gravity to follow a straight line. Indeed, the path followed by the glideslope algorithm would be a feasible path for the MPC optimizations, but they have found paths with lower fuel cost, moving nearer to the edges of the visibility constraint cone.

Comparison including Disturbance

This section compares the glideslope algorithm with RVH-MPC when disturbances are included in the simulation. The disturbance environment is discussed in the 'Test Case Description' section and the configuration of the RVH-MPC is described in the 'Controller Formulations' section. Table 2 shows the fuel use for four different runs of each simulation. Each run has a different, randomly chosen disturbance profile within the specified bound.

Fig. 6 shows a comparison of the mean fuel use for each controller and test case. To illustrate sensitivity to the disturbance, the fuel-use with disturbance removed is also shown. As would be expected, all the controllers require greater fuel use in the presence of the disturbance. RVH-MPC uses 35% less fuel than the glideslope algorithm for case A and 33% less for case B.

Table 2: Simulation Results with Disturbance. Four separate simulations and the overall mean are shown for each test. *ΔV in m/s.

Controller	Case A ΔV*	Case B ΔV
Glideslope	0.226	0.486
	0.234	0.480
	0.233	0.481
	0.233	0.483
Mean	0.232	0.482
RVH-MPC	0.161	0.321
	0.155	0.324
	0.150	0.330
	0.142	0.319
Mean	0.152	0.323

Robust Completion Demonstration

Fig. 7 shows the paths of six approaches for case (B) under RVH-MPC. Each is different due to the random disturbance, but all reach the target. Fig. 8 shows the change in cost from each plan to the next for one such approach. The cost is always decreasing and the rate remains below the predicted bound from (18). This demonstrates that the robust completion property (18) holds.

CONCLUSIONS

The new Model Predictive Control formulation, using Mixed-Integer Linear Programming to effect a variable planning horizon, has been shown to offer fuel savings in the performance of rendezvous between spacecraft. Simulations were performed to investigate performance in both radial and in-track approaches to the target, comparing with both the currently-favored glideslope algorithm and an earlier MPC formulation. MPC is an improvement over the glideslope algorithm because it includes an online minimum-fuel trajectory optimization, allowing it to find the best approach path within constraints of sensor visibility and safety. The advantage of the new MPC formulation over earlier MPC schemes is its ability to handle general target constraints and cost functions. The new method also guarantees robust finite-time completion. Simulations

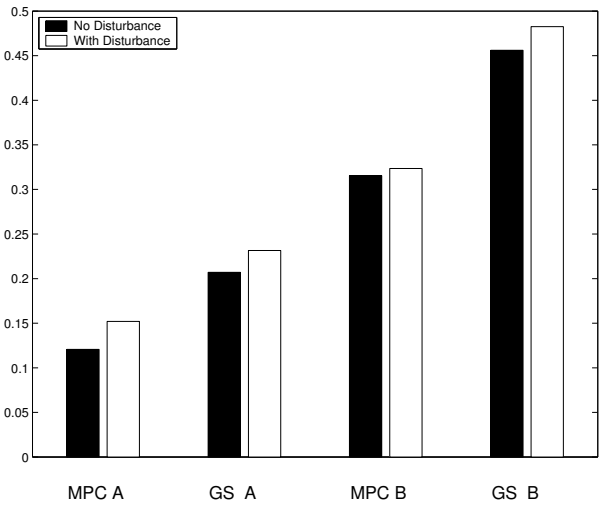

Fig. 6: Comparison of Fuel Use of Glideslope (GS) and RVH-MPC with and without Disturbance. Fuel figures for tests with disturbances are the mean values of four simulations.

including unmodeled disturbances have shown that the MPC optimization is always feasible and that the predicted bound on the rate of cost decrease is valid. These simulations also showed that MPC maintains its performance advantage over the glideslope method when uncertainty is included.

ACKNOWLEDGMENTS

Research funded in part by NASA CETDP grant # NAG5-10440.

REFERENCES

[1] I. Kawano, M. Mokuno, T. Kasai, T. Suzuki, "Result of Autonomous Rendezvous Docking Experiment of Engineering Test Satellite-VII," *Journal of Spacecraft and Rockets*, Vol. 38, No. 1, January 2001, AIAA, Reston, VA, pp. 105–111.

[2] A. G. Richards, J. P. How, "Model Predictive Control of Vehicle Maneuvers with Guaranteed Completion Time and Robust Feasibility," submitted to ACC 2003.

[3] D. Waltz, *On-Orbit Servicing of Space Systems*, Krieger Publishing, FL, 1993, pp. 193–227.

[4] M. E. Polites, "An Assessment of the Technology of Automated Rendezvous and Capture in Space," NASA Technical Report, No. TP-1998-208528, NASA MSFC, July 1998

[5] DARPA Orbital Express Website, `www.darpa.mil/tto/PROGRAMS/astro.html`, April 2002

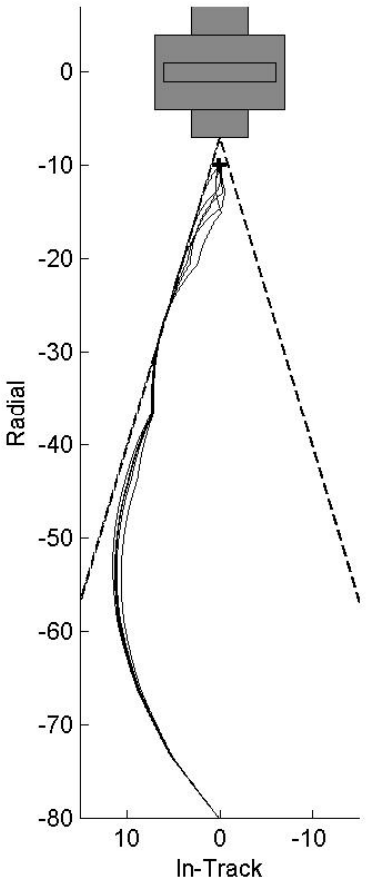

Fig. 7: Paths of six approaches under robust MPC.

[6] NASA Shuttle Press Kit, "STS-98 Rendezvous and Docking Overview", `shuttlepresskit.com/STS-98/rendezvous13.htm`, visited June 2003.

[7] H. B. Hablani, M. Tapper, D. Dana-Bashian, "Guidance Algorithms for Autonomous Rendezvous of Spacecraft with a Target Vehicle in a Circular Orbit," Paper No. 2001-4393, AIAA GNC, August 2001.

[8] D. J. Pearson, "The Glideslope Approach," *Advances in the Astronautical Sciences*, American Astronautical Society Paper No. AAS 89-162, pp. 109-123.

[9] J.M. Maciejowski, *Predictive Control with Constraints*, Prentice Hall, England, 2002.

[10] A. Bemporad and M. Morari, "Control of Systems Integrating Logic, Dynamics, and Constraints," in *Automatica,* Pergamon / Elsevier Science, New York NY, Vol. 35, pp. 407–427, 1999.

[11] A. Richards, T. Schouwenaars, J. How, E. Feron,

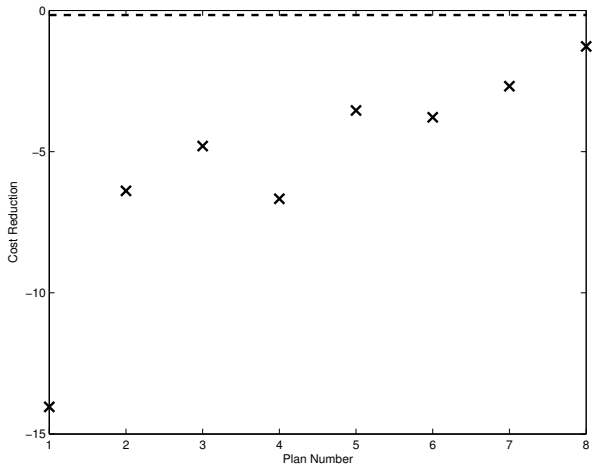

Fig. 8: Cost Change at Each Plan Step using Robust MPC. The dashed line is the predicted upper bound.

"Spacecraft Trajectory Planning With Collision and Plume Avoidance Using Mixed-Integer Linear Programming," *Journal of Guidance, Control and Dynamics*, AIAA, August 2002.

[12] R. Fourer, D. M. Gay, and B. W. Kernighar, *AMPL, A modeling language for mathematical programming,* The Scientific Press, 1993.

[13] *ILOG CPLEX User's guide*, ILOG, 1999.

[14] V. Manikonda, P. Arambel, M. Gopinathan, R. K. Mehra and F. Y. Hadaegh, "A Model Predictive Control-based Approach for Spacecraft Formation Keeping and Attitude Control," in *Proceedings of the American Control Conference*, June 1999, IEEE, Washington DC, pp 4258-4262.

[15] W. B. Dunbar, M. B. Milam, R. Franz and R. M. Murray, "Model Predictive Control of a Thrust-Vectored Flight Control Experiment," accepted for *15th IFAC World Congress on Automatic Control*, 2002

[16] D. Q. Mayne, J. B. Rawlings, C. V. Rao, P. O. M. Scokaert, "Constrained Model Predictive Control: Stability and Optimality," *Automatica*, 36(2000), Pergamon Press, UK, pp. 789–814.

[17] A. Bemporad, F. Borrelli and M. Morari, "Model Predictive Control Based on Linear Programming - The Explicit Solution," Technical Report AUT01-06, Automatic Control Laboratory, ETH Zentrum, 2001.

[18] V. Sakizlis, V. Dua, J. D. Perkins and E. N. Pistikopoulos, "The Explicit Control Law for Hybrid Systems via Parametric Programming," *American Control Conference*, Anchorage AK, AACC, 2002, p.674.

[19] M. H. Kaplan, *Modern Spacecraft Dynamics and Control,* Wiley, New York NY, 1976 pp 108–115.

[20] H. P. Rothwangl, "Numerical Synthesis of the Time Optimal Nonlinear State Controller via Mixed Integer Programming," IEEE *American Control Conference*, 2001.

[21] R. Franz, M. Milam, and J. Hauser, " Applied Receding Horizon Control of the Caltech Ducted Fan," ACC 2002.

[22] P. O. M. Scokaert, D. Q. Mayne and J. B. Rawlings, "Suboptimal Model Predictive Control (Feasibility Implies Stability)," *IEEE Transactions on Automatic Control*, Vol. 44 No. 3, 1999, p. 648.